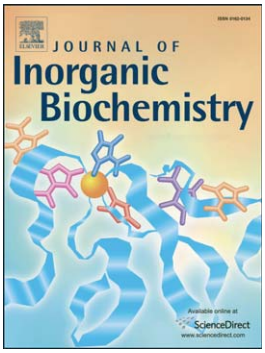

Diverse *in vitro* and *in vivo* anti-inflammatory effects of trichlorido-gold(III) complexes with N6-benzyladenine derivatives

Radka Křikavová, Jan Hošek, Pavel Suchý Jr., Ján Vančo, Zdeněk Trávníček

PII: S0162-0134(14)00041-5
DOI: doi: 10.1016/j.jinorgbio.2014.02.002
Reference: JIB 9468

To appear in: *Journal of Inorganic Biochemistry*

Received date: 21 November 2013
Revised date: 23 December 2013
Accepted date: 5 February 2014

Please cite this article as: Radka Křikavová, Jan Hošek, Pavel Suchý Jr., Ján Vančo, Zdeněk Trávníček, Diverse *in vitro* and *in vivo* anti-inflammatory effects of trichlorido-gold(III) complexes with N6-benzyladenine derivatives, *Journal of Inorganic Biochemistry* (2014), doi: 10.1016/j.jinorgbio.2014.02.002

Diverse *in vitro* and *in vivo* anti-inflammatory effects of trichlorido-gold(III) complexes with N6-benzyladenine derivatives

Radka Křikavová [a], Jan Hošek [a], Pavel Suchý, Jr. [b], Ján Vančo [a], Zdeněk Trávníček [a,*]

[a] *Regional Centre of Advanced Technologies and Materials, Department of Inorganic Chemistry, Faculty of Science, Palacký University in Olomouc, 17. listopadu 12, CZ-771 46 Olomouc, Czech Republic*

[b] *Department of Human Pharmacology and Toxicology, Faculty of Pharmacy, University of Veterinary and Pharmaceutical Sciences Brno, Palackého tř. 1/3, CZ-612 42 Brno, Czech Republic*

[*]Corresponding author. Tel.: +420 585 634 352; fax: +420585 634 954; e-mail: zdenek.travnicek@upol.cz (Zdeněk Trávníček).

Abstract

A series of gold(III) complexes involving differently substituted derivatives of a plant hormone N6-benzyladenine (HL1-5) is reported. The complexes have the general formula [Au(HL1-5)Cl_3]·*n*H_2O (n=0 for **1, 3**-**5**; and n=1 for **2**), where *N*6-(2-fluorobenzyl)adenine (HL1), *N*6-(2-chlorobenzyl)adenine (HL2), *N*6-(3-chlorobenzyl)adenine (HL3), *N*6-(4-chlorobenzyl)adenine (HL4) and *N*6-(4-methylbenzyl)adenine (HL5) represent the *N*9-coordinated ligands. The results of thorough characterization (elemental and thermal analyses, FT-IR, Raman and NMR spectroscopy, ESI+ mass spectrometry, conductivity measurements, DFT calculations) showed that the presented complexes **1**-**5** involve a central gold(III) atom coordinated in a square-planar geometry by the *N*9 atom of the purine moiety of HL1-5 and by three chlorido ligands. The complexes (**1**-**5**) were studied *in vitro* for cytotoxicity and anti-inflammatory activity on LPS-activated macrophages (THP-1 cell line), and *in vivo* for anti-inflammatory effects (**1**, **2**, **5**) using the carrageenan-induced hind paw oedema model on rats. Surprisingly, the results on the *in vitro* level revealed that the complexes show negligible cytotoxicity and anti-inflammatory activity, however, the activity on the *in vivo* level was found to be significant, fully comparable with the utilized drug Indomethacin, or even better as compared to a gold-containing metallodrug Auranofin.

Keywords: Gold(III) complexes; Adenine derivatives; TNF-α; Cytotoxicity; Anti-inflammatory.

1. Introduction

Medicinal applications of gold-based therapeutic agents have been well established since as early as 2500 BC [1, 2, 3]. Presently, the major clinical use of gold compounds is related to the treatment of a chronic inflammatory disease rheumatoid arthritis, which applies solely to compounds with gold in the oxidation state +I, e.g. Auranofin [triethylphosphine-(2,3,4,6-tetra-*O*-acetyl-*β*-D-thiopyranosato)-gold(I)] [4, 5, 6]. The current research interest in the medicinal chemistry of gold compounds is in particular connected with: *a*) the above-mentioned clinical success of gold(I) anti-inflammatory complexes and the efforts to find more efficient agents exhibiting fewer negative side-effects associated with the treatment (such as metallic taste in the mouth, discolouration of the skin, dermatitis, nausea, bone marrow damage, etc.); *b*) the unique chemistry of gold with respect to the physiological environment – particularly the high affinity for protein thiols and selenols, since many disease targets, including varied inflammatory illnesses, bone and joint disorders, parasitic diseases as well as cancer, involve cysteine residues [1]. In relation to this high affinity and distinctive metabolism of gold drugs, the possible medicinal application of gold compounds could be significantly widened, as suggested by recent studies and reviews focused on anti-microbial, anti-malaria, anti-cancer as well as anti-HIV activity [1, 2, 3, 7, 8].

The studies focused on development of potential gold-based drugs are mostly associated with the two oxidation states of gold, i.e. +I and +III, as they both can exist in physiological conditions. It has been well established that in the highly reductive environment *in vivo*, Au(I) species are much more stable than the Au(III) ones, which are readily reduced to Au(I) or Au(0) by naturally occurring reductants, such as thiols (cysteine), thioethers (methionine), and/or various proteins [1, 2, 6]. The fact that gold(III) can be readily reduced, and thus can act as a relatively strong oxidizing agent, has been connected in recent works with anti-HIV activity of various gold(III) complexes, as in this way the oxidation of target proteins/enzymes results in their functional inhibition [9]. However, it should be pointed out that the redox process could in certain conditions be reversible. As recent studies highlighted, the used Au(I) therapeutics should be in fact considered as pro-drugs. After

administration, they rapidly enter varied metabolic pathways, one of which involves oxidation of Au(I) to Au(III) by strong oxidants, such as hypochlorite which is produced in the oxidative environment in inflamed sites. Moreover, Au(III) has been suggested to dominate the anti-inflammatory as well as toxic actions of gold species [1,6].

While Au(I) compounds have already been successfully applied in clinic, recently a rising number of scientific studies has been devoted to Au(III) complexes. The majority of such studies have focused on the potential cytotoxic activity of gold(III) complexes [7, 8]. The chemical motivation behind this focus is rather straightforward – Au(III) is isoelectric with Pt(II), and its complexes generally adopt the square-planar geometry similarly to the widely used platinum-based anticancer drugs cisplatin and its derivatives. In recent years, the chemists have successfully overcome the low stability of gold(III) complexes under physiological conditions, connected with their oxidative properties and fast rate of hydrolysis, by introducing various chelating ligands [1,2]. For example, the compounds [Au(dmdt)X_2], [Au(esdt)X_2] [10,11], [AuY_2(damp)] [12,13] and [Au(tpp)]Cl [14,15], have shown significant antitumour activity *in vitro* as well as *in vivo* (dmdt = *N*,*N*-dimethyldithiocarbamate; esdt = ethylsarcosinedithiocarbamate; damp = 2-[(dimethylamino)methyl]phenyl; tpp = *meso*-tetraphenylporphyrin); X = Cl, Br; Y = Cl, acetate, malonate) [1].

The utilization of *N*6-benzyladenines as *N*-donor ligands, which are classified among natural as well as artificial plant hormones called cytokinins, may be associated with their biological functions. Their principal functions in the plant life cycle comprise the regulation of cell cycle, differentiation, division and senescence [16]. Moreover, some derivatives of *N*6-benzyladenine, such as *R*-roscovitine, 2-[(*R*)-(1-ethyl-2-hydroxyethylamino)]-*N*6-benzyl-9-isopropyladenine, have attracted further attention for their ability to influence the human cell cycle, particularly, in the cancer cells, thus exhibiting anti-tumour activity [17, 18]. In order to improve a biological activity, coordination compounds involving combinations of a suitable transition metal and *N*6-benzyladenine derivative are in the focus of research. The complexes involving such *N*-donor ligands have been shown to possess significant *in vitro* as well as *in vivo* anti-tumour (with the effective concentrations up to submicromolar level) [19,

20] and anti-diabetic activity [21]. Moreover, outstanding results concerning *in vitro* and *in vivo* anti-inflammatory activity have been recently reported for gold(I) complexes involving triphenylphosphine (PPh_3) and *N*6-benzyladenine (HL) derivatives in the coordination sphere, having the composition [Au(PPh_3)(L)]. The described complexes showed similar or better anti-inflammatory effects as compared with the commercially applied drug Auranofin while being less cytotoxic *in vitro* [22].

In relation to the recently reported high anti-inflammatory activity of the Au(I)-PPh_3 complexes involving *N*6-benzyladenine derivatives, the generally oxidative environment in the inflamed sites and the suggested role of Au(III) species in the anti-inflammatory action of clinically applied gold-based drugs outlined above, we decided to prepare and thoroughly characterize the Au(III) complexes of *N*6-benzyladenine derivatives and further study their *in vitro* and *in vivo* anti-inflammatory activity on the models of LPS-stimulated THP-1 macrophage-like cell line and carrageenan-induced hind paw oedema model on rats.

2. Materials and Methods

2.1. Starting materials

Used chemicals and solvents were obtained from commercial sources (Sigma-Aldrich Co., Acros Organics Co., Lachema Co. and Fluka Co.) and were used without any further purification. The organic compounds *N*6-(2-fluorobenzyl)adenine (HL1), *N*6-(2-chlorobenzyl)adenine (HL2), *N*6-(3-chlorobenzyl)adenine (HL3), *N*6-(4-chlorobenzyl)adenine (HL4) and *N*6-(4-methylbenzyl)adenine (HL5) (see Scheme S1) were synthesized according to the previously published procedure [23]. The identity and purity of these organic compounds were checked by elemental analysis (C, H, N), FT-IR and ^{1}H and ^{13}C NMR spectroscopy.

Scheme 1

2.2. Synthesis of Au(III) complexes

1 mmol of the corresponding *N*6-benzyladenine derivative (HL1-5) in acetone (70 mL) was added to a solution of 1 mmol of $AuCl_3$ in acetone (10 mL). The resulting solution was stirred for 4 h after which it was filtered. The obtained red filtrate was further stirred for about 30 min. Then the volume of the solution was reduced on the rotary evaporator until a red suspension formed. The red or dark red products were filtered off, washed with a small amount of acetone and diethyl ether, and dried at 40 °C under an infrared lamp.

$[Au(HL1)Cl_3]$(**1**): Yield: 70%. Anal. Calc. for $C_{12}H_{10}N_5FCl_3Au$: C, 26.4; H, 1.8; N, 12.8; Cl, 19.5. Found: C, 26.0; H, 1.5; N, 12.3; Cl, 19,0%. Λ_M (DMF/methanol, S $cm^2\,mol^{-1}$): 7.9/5.7. ESI+ MS (methanol, *m/z*) 244 (calc. 244) $[HL1+H]^+$, 546 (546) $[M+H]^+$. IR (ν_{Nujol}/cm^{-1}): 546s, 473m ν(Au–N), 415w, 365vs ν(Au–Cl), 351w ν(Au–Cl), 347w ν(Au–Cl), 301w, 298w, 261w, 214w. IR (ν_{KBr}/cm^{-1}): 3430m ν(N–H), 3203w, 3162w, 3039w $\nu(C–H)_{ar}$, 2936w $\nu(C–H)_{al}$, 1615s $\nu(C=N)_{ar}$, 1591w, 1529w, 1426m $\nu(C=C)_{ar}$, 1365m, 1301w, 1261m $\nu(C–F)_{ar}$, 1227w, 1098w, 982w, 832w, 790w, 653m. Raman (cm^{-1}): 3067m $\nu(C–H)_{ar}$, 2954w $\nu(C–H)_{al}$, 1609m $\nu(C=N)_{ar}$, 1552w, 1415m $\nu(C=C)_{ar}$, 1290m, 1229m $\nu(C–F)_{ar}$, 1180m, 1145w, 1035m, 951w, 775w, 565w, 408w, 318 s ν(Au–Cl), 253m, 168s. ^{1}H NMR (400.00 MHz, DMF-d_7, ppm): δ ($SiMe_4$) 8.15 (s, C2H, 1H), 7.96 (s, C8H, 1H), 7.77 (tt, 7.9 Hz, 1.6 Hz, C14H, 1H), 7.30, (qq, 7.5 Hz, 1.6 Hz, C15H, 1H), 7.18 (d, 9.2 Hz, C12H, 1H), 7.13 (t, 7.5 Hz, C13H, 1H), 4.98 (bs, C9H, 2H). ^{13}C NMR (75.43 MHz, DMF-d_7, ppm): δ ($SiMe_4$) 160.05 (C11), 155.39 (C6), 151.53 (C2), 148.52 (C8), 145.25 (C4), 133.09, 133.06 (C14), 132.67, 132.47 (C15), 129.21(C10), 124.82, 124.79 (C13), 120.96 (C5), 115.64, 115.43 (C12), 38.15 (C9).

$[Au(HL2)Cl_3]\cdot H_2O$ (**2**): Yield: 75%. Anal. Calc. for $C_{12}H_{12}N_5OCl_4Au$: C, 24.8; H, 2.1; N, 12.1; Cl, 24.4. Found: C, 24.7; H, 1.7; N, 11.9; Cl, 24.3%. Λ_M (DMF/methanol, S cm^2 mol^{-1}): 13.2/8.7. ESI+ MS (methanol, *m/z*) 260 (calc. 260) $[HL2+H]^+$, 564 (564) $[Au(HL2)Cl_3+H]^+$. IR (ν_{Nujol}/cm^{-1}): 591vs, 561m, 463s ν(Au–N), 433m, 364m ν(Au–Cl), 341w ν(Au–Cl), 306w, 275s, 260w. IR (ν_{KBr}/cm^{-1}): 3401m ν(N–H), 3274w, 3210w, 3114w, 3061w $\nu(C–H)_{ar}$, 2923w $\nu(C–H)_{al}$, 2854w, 1625vs $\nu(C=N)_{ar}$, 1574w, 1442w $\nu(C=C)_{ar}$, 1403m, 1358w, 1262m, 1172m, 1146w, 1038m $\nu(C–Cl)_{ar}$, 964w, 747m, 690w, 611w. Raman

(cm^{-1}): 3064m ν(C–H)$_{ar}$, 2918w ν(C–H)$_{al}$, 1616w, 1594m ν(C=N)$_{ar}$, 1573w, 1511m, 1406m ν(C=C)$_{ar}$, 1331w, 1291m, 1157m, 1039m ν(C–Cl)$_{ar}$, 992w, 804w, 759m, 738m, 690w, 542w, 413m, 346vs ν(Au–Cl), 322vs ν(Au–Cl). ^{1}H NMR (400.00 MHz, DMF-d_7, ppm): δ (SiMe$_4$) 8.13 (s, C2H, 1H), 7.93 (s, C8H, 1H), 7.77 (d, 8.5 Hz, C12H, C15H, 2H), 7.36 (d, 8.5 Hz, C13H, C14H, 2H), 4.90 (bs, C9H, 2H). ^{13}C NMR (75.43 MHz, DMF-d_7, ppm): δ (SiMe$_4$) 155.38 (C6), 151.51 (C2), 148.44 (C8), 141.10 (C4), 138.10 (C10), 133.11 (C15), 133.07 (C12), 129.86 (C14), 120.92 (C5), 43.86 (C9).

[Au(HL3)Cl$_3$] (**3**): Yield: 65%. Anal. Calc. for $C_{12}H_{10}N_5Cl_4Au$: C, 25.6; H, 1.7; N, 12.4; Cl, 25.2. Found: C, 25.2; H, 1.6; N, 12.7; Cl, 24.8. Λ_M (DMF/methanol, S cm^2 mol^{-1}): 21.6/10.8. ESI+ MS (methanol, *m/z*) 260 (calc. 260) [HL3+H]$^+$, 564 (564) [M+H]$^+$, 586 (586) [M+Na]$^+$. IR (ν_{Nujol}/cm^{-1}): 596m, 565w, 539w, 448m ν(Au–N), 414w, 368s ν(Au–Cl), 338w ν(Au–Cl), 279w, 245w. IR (ν_{KBr}/cm^{-1}): 3384m ν(N–H), 3122w, 3066w ν(C–H)$_{ar}$, 2927w ν(C–H)$_{al}$, 2854w, 1619vs ν(C=N)$_{ar}$, 1563w, 1473m ν(C=C)$_{ar}$, 1404m, 1339m, 1278w, 1178m, 1144w, 1095w, 1078w ν(C–Cl)$_{ar}$, 956w, 871w, 778w, 684w. Raman (cm^{-1}): 3065m ν(C–H)$_{ar}$, 2936w ν(C–H)$_{al}$, 1618w ν(C=N)$_{ar}$, 1597m, 1571w, 1518w, 1445m, 1401m ν(C=C)$_{ar}$, 1334m, 1209w, 1167m, 1143w, 1078w ν(C–Cl)$_{ar}$, 999m, 929w, 751w, 681w, 548w, 415m, 367s ν(Au–Cl), 339vs ν(Au–Cl). ^{1}H NMR (400.00 MHz, DMF-d_7, ppm): δ (SiMe$_4$) 8.18 (s, C2H, 1H), 8.04 (s, C8H, 1H), 7.50 (t, 1.8 Hz, C11H, 1H), 7.42 (d, 7.6 Hz, C13H, 1H), 7.36 (t, 7.7 Hz, C14H, 1H), 7.29 (dd, 7.8, 1.8, C15H, 1H), 4.92 (bs, C9H, 2H). ^{13}C NMR (75.43 MHz, DMF-d_7, ppm): δ (SiMe$_4$) 155.15 (C6), 152.32 (C2), 148.18 (C8), 146.05 (C4), 144.49 (C10), 134.03 (C12), 130.70 (C14), 127.92 (C11), 127.25 (C15), 126.70 (C13), 120.01 (C5), 43.98 (C9).

[Au(HL4)Cl$_3$] (**4**): Yield: 75%. Anal. Calc. for $C_{12}H_{10}N_5Cl_4Au$: C, 25.6; H, 1.7; N, 12.4; Cl, 25.2. Found: C, 25.2; H, 1.9; N, 11.9; Cl, 25.5%. Λ_M (DMF/methanol, S cm^2 mol^{-1}): 37.3/15.5. ESI+ MS(methanol, *m/z*) 260 (calc. 260) [HL4+H]$^+$, 528 (528) [Au(I)(HL4)Cl+2H$_2$O+H]$^+$, 564 (564) [M+H]$^+$, 586 (586) [M+Na]$^+$. IR (ν_{Nujol}/cm^{-1}): 566m, 539m, 521m, 491m ν(Au–N), 407w, 359vs ν(Au–Cl), 329m ν(Au–Cl), 286w, 273m, 251w. IR (ν_{KBr}/cm^{-1}): 3425m ν(N–H), 3268w, 3119m ν(C–H)$_{ar}$, 2925w ν(C–H)$_{al}$, 2850w, 1629vs ν(C=N)$_{ar}$, 1546w, 1490m, 1450m ν(C=C)$_{ar}$, 1406m, 1358w, 1305w, 1269w, 1208w, 1169m, 1139w, 1091m ν(C–Cl)$_{ar}$, 1014m, 951w, 801w, 777w, 750w, 637w, 598w, 543w. Raman (cm^{-1}): 3087s ν(C–H)$_{ar}$, 2942w

ν(C–H)$_{al}$, 1618m ν(C=N)$_{ar}$, 1599m, 1528m, 1428m ν(C=C)$_{ar}$, 1327w, 1220m, 1227w, 1123w, 1027m ν(C–Cl)$_{ar}$, 928w, 727w, 634w, 587w, 367m, 336m ν(Au–Cl). ^{1}H NMR (400.00 MHz, DMF-d_7, ppm): δ ($SiMe_4$) 8.15 (s, C2H, 1H), 7.48 (d, 8.6 Hz, C11H, C15H, 2H), 7.39 (s, C8H, 1H), 7.38 (d, 8.6 Hz, C12H, C14H, 2H), 4.89 (bs, C9H, 2H). ^{13}C NMR (75.43 MHz, DMF-d_7, ppm): δ ($SiMe_4$) 155.34 (C6), 152.49 (C2), 148.45 (C8), 144.05 (C4), 140.82 (C10), 132.21 (C13), 128.87 (C12,14), 121.06 (C5), 43.83 (C9).

[Au(HL5)Cl_3] (**5**): Yield: 78%. Anal. Calc. for $C_{13}H_{13}N_5Cl_3Au$: C, 28.8; H, 2.4; N, 12.9; Cl, 19.6. Found: C, 28.4; H, 2.6; N, 13.2; Cl, 19,9%. Λ_M (DMF/methanol, S cm^2 mol^{-1}): 18.8/17.1. ESI+ MS (methanol, *m/z*) 240 (calc. 240) [HL5+H]$^+$, 542 (542) [M+H]$^+$. IR (ν_{Nujol}/cm^{-1}): 557s, 532m, 490m ν(Au–N), 400w, 362vs ν(Au–Cl), 342w ν(Au–Cl), 318w ν(Au–Cl), 287m, 213w. IR (ν_{KBr}/cm^{-1}): 3405m ν(N–H), 3210m, 3060m ν(C–H)$_{ar}$, 2939m, 2918w ν(C–H)$_{al}$, 2824m ν(C–H)$_{met}$, 1617vs ν(C=N)$_{ar}$, 1514w, 1438m ν(C=C)$_{ar}$, 1301m, 1256w, 1157w, 1021w, 934w, 809w, 731w, 626m, 590w. Raman (cm^{-1}): 3115w, 3043s ν(C–H)$_{ar}$, 2992m, 2932w ν(C–H)$_{al}$, 1615w ν(C=N)$_{ar}$, 1559w, 1424m ν(C=C)$_{ar}$, 1373w, 1315vs, 1173w, 999vs, 799w, 741m, 582m, 536w, 420w, 337s, 355m ν(Au–Cl). ^{1}H NMR (400.00 MHz, DMF-d_7, ppm): δ ($SiMe_4$) 8.19 (s, C2H, 1H), 7.39 (s, C8H, 1H), 7.34 (d, 8.6 Hz, C11H, C15H, 2H), 7.28 (d, 8.6 Hz, C12H, C14H, 2H), 4.89 (bs, C9H, 2H), 2.30 (s, C13'H, 3H). ^{13}C NMR (75.43 MHz, DMF-d_7, ppm): δ ($SiMe_4$) 155.34 (C6), 152.49 (C2), 148.45 (C8), 144.05 (C4), 140.82 (C10), 133.03 (C11,15), 132.21 (C13), 128.87 (C12,14), 121.06 (C5), 43.83 (C9), 20.21 (C13).

2.3. General methods of characterization

Elemental analyses (C, H, N) were performed on a Flash 2000 CHNO-S Analyser (Thermo Scientific). The chlorine content was determined by the Schöniger method [24]. Conductivity measurements of 10^{-3} M *N,N´*-dimethylformamide (DMF) and 10^{-3} M methanol solutions of the prepared complexes were carried out using a conductometer 340i/SET (WTW) at 25 °C. FT-IR spectra were recorded on a Nexus 670 FT-IR spectrometer (ThermoNicolet) using KBr pellets (400-4000 cm^{-1}) and the Nujol technique (150-600 cm^{-1}). Raman spectrometer Nicolet NXR 9650 equipped with the liquid nitrogen cooled NXE Genie germanium detector (ThermoNicolet) was used to record Raman

spectra of all the complexes (150-4000 cm^{-1}). The reported FT-IR and Raman signal intensities are defined as w = weak, m = middle, s = strong and vs = very strong. ^{1}H and ^{13}C NMR spectra of the DMF-d_7 solutions were measured on a Varian 400 MHz NMR spectrometer at 300 K. Tetramethylsilane (TMS) was used as an internal reference standard for ^{1}H and ^{13}C NMR experiments. Mass spectra of the methanol solutions of the complexes were obtained by an LCQ Fleet ion trap mass spectrometer by the positive mode electrospray ionization (ESI+) technique (Thermo Scientific). The theoretic values were calculated by the QualBrowser software (version 2.0.7, Thermo Fisher Scientific). Thermogravimetric (TG) and differential thermal analyses (DTA) were performed using a thermal analyser Exstar TG/DTA 6200 (Seiko Instruments Inc.) in dynamic air conditions (150 mL min^{-1}) between room temperature (≈25 °C) and 900 °C (gradient 2.5 °C min^{-1}).

2.4. Biological activity testing

2.4.1. Chemicals and biochemicals

The RPMI 1640 medium and penicillin-streptomycin mixture were purchased from Lonza (Verviers, Belgium). Phosphate-buffered saline (PBS), foetal bovine serum (FBS), phorbol myristate acetate (PMA), prednisone (98%≤), and *Escherichia coli* 0111:B4 lipopolysaccharide (LPS) were purchased from Sigma-Aldrich (Steinheim, Germany). The Cell Proliferation Reagent WST-1 was obtained from Roche (Mannheim, Germany). An Instant ELISA Kit (eBioscience, Vienna, Austria) was used to evaluate the production of TNF-α.

2.4.2. Maintenance and preparation of macrophages

For the measurements of biological activity, we used the human monocytic leukemia cell line THP-1 (ECACC, Salisbury, UK). The cells were cultivated at 37 °C in RPMI 1640 medium supplemented with 2 mM L-glutamine, 10% FBS, 100 U/mL of penicillin and 100 μg/mL of streptomycin in a humidified atmosphere containing 5% CO_2. Stabilized cells (3^{rd}–15^{th} passage) were split into microtitration plates to get a concentration of 500 000 cells/mL and the differentiation to

macrophages was induced by a phorbol myristate acetate (PMA) dissolved in dimethyl sulfoxide (DMSO) at the final concentration of 50 ng/ml and the cells were incubated for 24 h. In comparison with monocytes, differentiated macrophages tend to adhere to the bottoms of the cultivation plates. For the next 24 h the cells were incubated with fresh complete RPMI medium, i.e. containing antibiotics and FBS, without PMA. The medium was then aspirated, and the cells were washed with PBS and cultivated for next 24 h in a serum-free RPMI 1640 medium. These prepared macrophages were used for the detection of inflammatory response.

2.4.3. Cytotoxicity testing

THP-1 cells (floating monocytes, 500 000 cells/mL) were seeded into 96-well plates in triplicate and cultivate in a serum-free RPMI 1640 medium at 37 °C. Measurements were taken 24 h after the treatment with an increasing concentration of the tested compounds dissolved in DMSO. Viability was measured by the WST-1 test according to the manufacturer's manual. The amount of created formazan (which correlates to the number of metabolically active cells in the culture) was calculated as a percentage of control cells, which were treated only with DMSO and was set-up as 100%.

2.4.4. Drug treatment and induction of inflammatory response

Differentiated macrophages were pre-treated for 1 h either with a 5 µM solution of the tested complexes or uncoordinated organic compounds (HL1-5), or 5 µM solution of prednisone, or 5 µM $AuCl_3$ dissolved in DMSO (the final DMSO concentration was 0.1%) or with 0.1% DMSO solution itself (*vehicle*); the tested compounds lack a cytotoxic effect at the given concentration (cell viability >94%). The inflammatory response was triggered by adding 1.0 µg/mL lipopolysaccharide (LPS) dissolved in water to the pre-treated macrophages, *control* cells were without the LPS treatment. Each experiment was repeated three times.

2.4.5. Evaluation of cytokine secretion by ELISA

Macrophages, which were pre-treated with the tested compounds for 1 h, were incubated with LPS for next 24 h. After this period, the medium was collected and the concentration of TNF-α was measured by an Instant ELISA kit according to the manufacture's manual.

2.4.6. Animals

Wistar - SPF (6-8 weeks male) rats were obtained from AnLab, Ltd. (Prague, Czech Republic). The animals were kept in plexiglass cages at the constant temperature of 22±1 °C, and relative humidity of 55±5% for at least 1 week before the experiment. They were given food and water *ad libitum*. All experimental procedures were performed according to the National Institutes of Health (NIH) Guide for the Care and Use of Laboratory Animals. In addition, all tests were conducted under the guidelines of the International Association for the Study of Pain [25]. After a one-week adaptation period, male Wistar-SPF rats (200-250 g) were randomly assigned to six groups (n = 10) of animals in the study. The treated groups received the solutions of complexes **1**, **2**, and **5** (*intraperitoneally, i.p.*) dissolved in 25% DMSO (*v/v* in water for injections according to the European Pharmacopoeia, PhEur, rules). The next three groups included a carrageenan-treated (control group), Auranofin positive control (Auranofin + carrageenan) and Indomethacin positive control groups (Indomethacin + carrageenan).

2.4.7. Carrageenan-induced hind paw oedema model

The carrageenan-induced hind paw oedema model was used for the determination of anti-inflammatory activity [26]. Animals were *i.p*. pre-treated with complexes **1**, **2** and **5** (10 mg/kg), Auranofin (10 mg/kg), Indomethacin (5 mg/kg) or 25% DMSO (*v/v* in water for injections PhEur), 30 min prior to the injection of 1% λ-carrageenan (50 μL) into the plantar side of right hind paws of the rats. The paw volume was measured immediately after carrageenan injection and during the next 6 h after the administration of the oedematogenic agent using a plethysmometer (model 7159, Ugo

Basile, Varese, Italy). The degree of swelling induced was calculated as the percentage of the change in the right hind paw volume after the carrageenan treatment from the initial right hind paw volume before the treatment. The anti-inflammatory drugs Auranofin and Indomethacin were used as positive controls.

3. Results and Discussion

3.1. Syntheses and general characterization of the Au(III) complexes

Red or dark red complexes of the formulas $[Au(HL1)Cl_3]$ (**1**), $[Au(HL2)Cl_3]\cdot H_2O$ (**2**), $[Au(HL3)Cl_3]$ (**3**), $[Au(HL4)Cl_3]$ (**4**) and $[Au(HL5)Cl_3]$ (**5**), where HL1-5 stand for the electroneutral form of the corresponding benzyl-substituted derivatives of *N*6-benzyladenine, namely *N*6-(2-fluorobenzyl)adenine (HL1), *N*6-(2-chlorobenzyl)adenine (HL2), *N*6-(3-chlorobenzyl)adenine (HL3), *N*6-(4-chlorobenzyl)adenine (HL4) and *N*6-(4-methylbenzyl)adenine (HL5) are reported. The complexes were synthesized by the reactions of $AuCl_3$ and the corresponding organic compound in the molar ratio of 1:1 in acetone (Scheme 1). The obtained compounds were thoroughly characterized by elemental analysis, FT-IR, Raman and NMR spectroscopy, ESI+ mass spectrometry, thermogravimetric (TG) and differential thermal (DTA) analyses. Multiple efforts were performed in order to prepare single crystals of the complexes **1**-**5** suitable for X-ray analysis. Apart from recrystallization of the powder products from DMSO, DMF, methanol or combination of these solvents and slow evaporation of these solutions as well as of mother liquors after syntheses at room temperature or 5 °C, diffusion crystallization methods were applied with varied combination of solvents (diffusion of diethyl ether, ethanol). However, none of these techniques led to the preparation of single crystals suitable for X-ray analysis.

The complexes **1**-**5** are well soluble in DMSO, DMF and methanol. The conductivity measurements were performed for the 10^{-3} M methanolic as well as DMF solutions of the complexes **1**-**5**, which proved that they behave as nonelectrolytes (Λ_M, DMF/methanol: 7.9-37.3/5.7-15.5 S cm^2 mol^{-1}).

Simultaneous TG and DTA analyses provided evidence that the presented complexes are thermally stable up to 155 °C and are non-solvated apart from complex **2** which is solvated by one water molecule of crystallization. The weight loss observed on the TG curve (∆m: calc. 3.0 / found 2.8%) associated with the loss of one crystal water molecule for complex **2** was accompanied by a small *endo*-effect at 149 °C on the DTA curve. The dehydration was finished at 155 °C. No stable intermediates formed during the thermal decay of all the complexes, which was finished by the formation of elemental gold at 747-908 °C. The differences between the overall weight losses determined by the thermal analyses and those calculated to Au as the final product of thermal degradation did not exceed 1.8%. The figures showing the results of TG/DTA analyses of complexes **2** and **5** can be found in Supplementary material (Figure S2).

3.2. Infrared, Raman, NMR and mass spectral characterization

The courses of the infrared and Raman spectral curves of the complexes were qualitatively similar to those of the corresponding organic compounds HL1-5, which clearly demonstrated the presence of HL1-5 in the structures of **1**-**5**. The infrared spectra of purine compounds in general are characteristic by the presence of very intensive bands of the ν(C=N)$_{ar}$ ring vibrations in the region of 1600-1640 cm^{-1}, which were also detected in the spectra of **1**-**5** at 1615-1629 cm^{-1} [27]. The multiple bands observed between 1426 and 1591 cm^{-1} can be attributed to the ring ν(C=C)$_{ar}$ vibrations detected in the infrared as well as Raman spectra. Further peaks characteristic of the organic skeletons were also identified, i.e. the stretching ν(N–H), ν(C–H)$_{ar}$ and ν(C–H)$_{al}$ vibrations at 3384-3425 cm^{-1}, 3039-3162 cm^{-1}, and 2918-2939 cm^{-1}, respectively. The substitution of hydrogen on the benzene ring of HL1-5 was confirmed by the presence of the bands assignable to ν(C–F)$_{ar}$ (at 1261 cm^{-1}), ν(C–Cl)$_{ar}$ (1038-1091 cm^{-1}) and ν(C–H)$_{met}$ (at 2824 cm^{-1}). The spectra measured in the far infrared region revealed several new peaks as compared to the spectra of the corresponding free organic molecules HL1-5. The peaks assignable to ν(Au–N) were found at 463-491 cm^{-1}. The previously published studies report that complexes of the type [Au(L)Cl$_3$] (where L stands for heterocyclic *N*-

donor ligands) showed three bands in the far-IR region connected with the vibrational modes of Au–Cl; the asymmetric *v*(Au–Cl) of the chlorine atoms *trans* to each other (at ca. 350-360 cm^{-1}), the symmetric *v*(Au–Cl) vibration (ca. 340 cm^{-1}) and *v*(Au–Cl) of the chlorine *trans* to the L ligand (310-320 cm^{-1}). The asymmetric stretching of the Cl–Au–Cl group and *v*(Au–Cl) *trans* to L might also overlap. In concordance with these findings, strong to medium intensity bands at 359–354 cm^{-1} and weak bands at 329-347 cm^{-1} were detected in the infrared spectra of **1**-**5** [28,29].

The obtained results of NMR experiments gave evidence of the composition of the gold(III) complexes. The most important coordination shifts ($\Delta\delta = \delta_{complex} - \delta_{ligand}$) are summarized in Table 1. The signals observed in the ^{1}H NMR spectra for the hydrogen atoms bound to the C2 and C8 atoms were shifted by 0.04-0.12 ppm upfield, and 0.17-0.81 ppm upfield, respectively. The highest coordination shifts of carbon atoms were determined for the C4 and C8 atoms, i.e. the closest vicinity of N9, which were shifted by 4.83-10.27 ppm to lower frequencies, and 8.33-8.86 ppm to higher frequencies, respectively (see Table 1). Considerable coordination shifts were also detected for the signals assigned to the C5 atom, which were observed moved by 0.99-1.78 ppm downfield. These resulting shifts are consistent with the suggested coordination of the organic compounds HL1-5 via the N9 atom in the complexes **1**-**5**. It should be noted, that another possible coordination site is represented by N7 as seen in Au(III) complexes involving a purine derivative, whose X-ray structures have been determined so far, i.e. [$AuCl_3$(1,9-diMeGua)], [$AuCl_3$(O6-Me-9-MeGua)] [30] and [Au(Hdamp-C^1)Cl(Spur)]Cl [31], where 1,9-diMeGua = 1,9-dimethylguanine; O6-Me-9-MeGua = O6,9-dimethylguanine, HSpur = 6-merkaptopurine and Hdamp-C^1 = 2-(dimethylaminomethyl)benzene. The coordination proceeds via N7, since the N9 site is blocked by methyl substitution in the guanine derivatives and deprotonated 6-merkaptopurine coordinates in a stable N7,S-chelating mode. On the other hand, N9-coordination is suggested in Au(III) complex involving adenine, i.e. in [$AuCl_3$(Ade)], based on results following from a combination of spectral techniques [32]. Accordingly, NMR data clearly confirm the N9-coordination of the adenine-derived HL1-5 ligands. Additionally, the observed chemical shifts comply also with the change in the protonation pattern, i.e. a change in the

tautomeric form of HL1-5. While the most populated tautomer of uncoordinated HL1-5 is represented by the form with a hydrogen atom bonded to the nitrogen atom N9 (the N9-H tautomer), the coordination of these molecules to Au(III) leads to a shift from the N9-H tautomer to the second most favourable N7-H tautomer in **1**-**5**. Such shifts of tautomer equilibria introduced by metal binding, or in other words, metal-stabilization of less favourable tautomers, have been well documented for nucleobases [33].

Table 1

ESI+ mass spectrometry proved to be a very useful tool in aiding to elucidate the structural aspects of the prepared complexes **1**-**5**, as the molecular peaks $[M+H]^+$ were detected for all the presented complexes thus supporting the suggested compositions. The mentioned $[M+H]^+$ molecular peaks were found in the 546-564 *m/z* region for **1**-**5**, while additionally, in the cases of **3** and **4**, the peaks of the $[M+Na]^+$ adducts with the sodium ion were observed at 586 *m/z*. All the mass spectra of **1–5** contained the fragment corresponding to the relevant *N*6-benzyladenine derivative, i.e. $[HL1\text{-}5+H]^+$. In the case of complex **4**, also a pseudomolecular ion corresponding to the reduced species of the composition $[Au(I)(HL4)Cl+2H_2O+H]^+$ was identified in the ESI+ mass spectrum. Supplementary material contains figure Figure S1 displaying the ESI+ mass spectrum of complex **4**.

3.3. Quantum chemical calculations

The multiple efforts to prepare single crystals of the presented complexes were unsuccessful. That is why, in the endeavour to confirm the composition of **1**-**5** arising from the indirect analytical methods described above and to predict the molecular structure of **1**, the results of spectroscopic and other analyses were summarized, together with the known structures of similar complexes, and the built model was optimized at the DFT-level of theory using the hybrid B3LYP functional with the LACVP+* basis set using a Spartan´10 (version 1.1.0v4) software [34,35,36]. The optimized geometry of complex **1** is shown in Figure 1. The gold(III) atom is tetra-coordinated by one *N*9-coordinated *N*6-(2-fluorobenzyl)adenine (Au1−N9 = 2.084 Å) and by three chloride ligands (Au1−Cl1 = 2.324 Å,

Au1−Cl2 = 2.378 Å and Au1−Cl3 = 2.381 Å). Only 18 tetra-coordinated [Au(L)Cl_3] complexes, where L represents an organic ligand coordinated via a heterocyclic nitrogen atom, have been deposited within the Cambridge Structural Database (version 5.34, update May 2013) [37]. A comparison of bond distances showed that the calculated Au–N bond length (Au1−N9 = 2.084 Å) is well comparable with those crystallographically determined [1.980(20)–2.107(10) Å]. On the other hand, the calculated Au–Cl bond lengths were found to be slightly longer, as they equal 2.324–2.381 Å as compared to 2.195(11)–2.363(2) Å for the CSD-deposited compounds. This might be connected with the fact that the calculations of the optimized geometry were performed in vacuum. The geometry around the gold(III) atom can be described as distorted square-planar; the angles Cl1–Au–N9, and Cl2–Au–Cl3 which are equal to 179.63°, and 175.65°, respectively.

Figure 1

3.4. In vitro cytotoxicity

The cytotoxic effects of the tested complexes **1**-**5** as well as of uncoordinated N6-benzyladenine derivatives HL1-5 were evaluated on the THP-1 cell line. None of the used compounds showed a cytotoxic effect up to the concentration of 20 μM. The lowest observed viability (84 % ± 6 %) was found for complex **5** at the concentration of 20 μM. Previously prepared Au(I) complexes also involving benzyl-substituted derivatives of N6-benzyladenine [22] showed EC_{50} lower than 2.5 μM. This comparison indicates higher cytotoxic potential of the Au(I) complexes of *N*6-benzyladenine derivatives than the Au(III) ones. Similar observation was reported by Sivaram et al. [38] whose work compared cytotoxicity of Au(I) and Au(III) complexes bearing benzimidazole- and pyrazole-derived carbenes on the NCI-H1666 non-small cell lung cancer cell line.

Cytotoxicity as well as further anti-inflammatory activity testing was performed in DMSO. In order to confirm the stability of the tested complexes in this solvent, time-dependent ^{1}H NMR spectra of representative complex **1** were measured in DMSO. The obtained results clearly showed that the complex behaves in DMSO solutions quite similarly as in DMF solutions (as described above),

as the character of the spectra was analogical. Moreover, even after 48 hours no significant shift, splitting or appearance of new peaks (connected with the coordination of DMSO) were observed. Based on these results, we can propose that the title complexes are stable in DMSO solutions in the time span of the biological testing.

3.5. In vitro anti-inflammatory effect

Gold containing complexes are known for their anti-inflammatory potential. However, these properties have been primarily studied for compounds with gold in the oxidation state (+I). Yet, multiple works dealing with the mechanism of action of Au(I) anti-inflammatory drugs suggest that one possible metabolic pathway of gold(I) species could involve oxidation of Au(I) to Au(III) in the highly oxidative environment in the inflamed sites. We have recently reported significant anti-inflammatory potential of Au(I) complexes involving N6-benzyladenine derivatives [22]. In order to verify if this biological effect could be observed also for the Au(III) complexes involving similar ligands, we determined the ability of the herein presented complexes **1**-**5** to attenuate the LPS-induced TNF-α secretion in macrophage-like cell line THP-1 (Figure 2). The obtained results indicated a moderate effect of the tested complexes on the TNF-α secretion attenuation, but the effect was lower than for positive control prednisone. Au(III) complexes showed a highly decreased anti-inflammatory effect in comparison with the previously published Au(I) complexes bearing similar ligands [22].

For comparison, we also tested the starting compounds, i.e. the uncoordinated organic compounds HL1-5 and $AuCl_3$. It was shown that only $AuCl_3$ significantly attenuated production of TNF-α, while the free HL1-5 ligands exhibited no effect.

Figure 2

3.6. The effect of Au(III) complexes on carrageenan-induced oedema in vivo

The *in vivo* tests of anti-inflammatory activity were inspired by the previous very positive results of anti-inflammatory activity demonstrated by the gold(I) complexes, [Au(L)(PPh_3)], involving triphenylphosphine and similar *N*-donor ligands [22]. The other reason for realization of the *in vivo* experiments was based on the results of *in vitro* testing, which revealed reasonable *in vitro* anti-inflammatory activity of the tested gold(III) complexes. From the group of five gold(III) complexes (**1**–**5**), three were chosen (**1**, **2**, **5**) to fulfil the requirements of the principle of three R´s (the principles of reduction, refinement and replacement on which all animal testing is based) and also to open the possibility to at least qualitatively evaluate the effect of substitution of the *N*-donor ligands on the anti-inflammatory activity *in vivo*. For these reasons, the complexes **1**, **2** and **5** were selected for the pre-treatment of laboratory animals in the carrageenan-induced hind paw oedema model on rats. In this experiment, the effects of the tested complexes on one of the symptoms of acute inflammation (*i.e*. the formation of oedema) were investigated. Due to the similar chemical composition and intended purpose, we chose Auranofin as the primary standard of anti-inflammatory activity. According to the literature, it has been used in biological experiments in diverse dosage regimen. In our experiments, we used it in the same dosages as the tested compounds; at 10 mg/kg in the form of the fine suspension in 25% DMSO (v/v in water for injections PhEur) applied intraperitoneally 30 min before the intraplantar injection of λ-carrageenan solution. As a secondary standard, NSAID Indomethacin was used in the dose of 5 mg/kg and applied intraperitoneally. The changes in the hind paw volume were monitored plethysmometrically for 6 h after the carrageenan injection and calculated as percentual changes of the initial volume for every individual animal. The comprehensive overview of the antiedematous activity time-dependent profiles of the tested compounds is summarized in Figure 3.

Figure 3

The highest activity was found for complex **1**, whose time-dependent profile of anti-oedematous activity copied almost perfectly the profile of Indomethacin and proved to be significantly higher than Auranofin ($P<0.05$). As it turned out, however, the biggest drawback of complex **1** was its toxicity in the applied dose, leading to the sudden death of all animals 5 h after the injection of carrageenan. Complex **5** was less effective and less toxic than complex **1**, its activity profile was however shifted by about 5% upwards, especially in the middle stages of the experiment. It can be stated that, in general, its activity was comparable to Auranofin. Complex **2** showed only weak activity in this experiment.

Although it is complicated to objectively transform the results of this type of pharmacological experiment to numeric output useful for QSAR, we decided to describe the structure-activity relationship at least in a qualitative manner. It can be observed that there is an evident link between the hydrophobicity of the *N*-donor ligands (and probably also the complexes) and the results of anti-inflammatory activities determined both *in vitro* and *in vivo*. With the increasing lipophilicity, the biological effect decreases in the following order *N*6-(2-fluorobenzyl)adenine > *N*6-(4-methylbenzyl)adenine > *N*6-(2-chlorobenzyl)adenine. The increase in lipophilicity of complexes can also have various side-effects on different physical properties (such as lowering of solubility) which can interfere with the bioavailability of complexes from biologically applicable vehicles.

4. Conclusions

A series of new gold(III) complexes (**1**-**5**) with benzyl-substituted derivatives of *N*6-benzyladenine (HL1-HL5) of the general formula $[Au(HL1\text{-}5)Cl_3]\cdot nH_2O$ (n=0 for **1, 3**-**5**; and n=1 for **2**) was prepared and characterized. The complexes were tested *in vitro* for their cytotoxic and anti-inflammatory activity on LPS-activated macrophages derived from the THP-1 cell line. The complexes were shown to be non-cytotoxic up to the concentration of 20 μM. The results of the *in vitro* testing evaluating the ability of the complexes to influence the LPS-induced TNF-α secretion in macrophage-like THP-1 cell line showed that the compounds only moderately attenuated the secretion.

Representative complexes **1**, **2** and **5** were tested for their anti-inflammatory activity *in vivo* on the carrageenan-induced hind paw oedema model on rats. The anti-oedematous activity was the most pronounced for complex **1** involving *N*6-(2-fluorobenzyl)adenine, as its activity was comparable with Indomethacin and significantly better than Auranofin. The positive *in vivo* anti-inflammatory action of complex **1** was negatively affected by a finding that the complex showed considerable toxicity, which decreases the possibility of the utilization of this complex as a gold-containing metallodrug. On the contrary, the results confirmed that the remaining complexes deserve deeper attention and study to understanding mechanisms of action and relationships between the structure and anti-inflammatory activity.

Acknowledgment

We acknowledge the financial support from the Operational Program Research and Development for Innovations - European Regional Development Fund (CZ.1.05/2.1.00/03.0058), the Operational Program Education for Competitiveness European Social Fund (CZ.1.07/2.3.00/20.0017) of the Ministry of Education, Youth and Sports of the Czech Republic and Palacký University (PrF_2013_015) for financial support. The authors thank Dr. Roman Buchtík for the mass spectra measurements, Dr. Pavel Štarha for TG/DTA experiments, and Mr. Tomáš Šilha for performing synthetic optimizations.

Appendix A. Supplementary material

The supplementary material file associated with this article contains the structural formulas of the *N*6-benzyladenine derivatives HL1−5 (Scheme S1), figures depicting the ESI+ mass spectrum of complex **4** (Figure S1) and TG/DTA curves for the complexes **2** and **5** (Figure S2). Supplementary data can be found, in the online version of this article, at doi:

References

[1] N.J. Farrer, P.J. Sadler, in: E. Alessio (Ed.), Bioinorganic Medicinal Chemistry, Wiley-VCH, Weinheim, Germany, 2011, pp. 1-48.

[2] M. Gielen, E.R.T. Tiekink, Metallotherapeutic Drugs and Metal-based Diagnostic Agents, The Use of Metals in Medicine, John Wiley and Sons, Ltd., Chichester, England, 2005.

[3] S.J. Berners-Price, A. Filipovska, Metallomics 3 (2011) 863–873; doi:10.1039/C1MT00062D.

[4] W.F. Kean, I.R.L. Kean, Inflammopharmacology 16 (2008) 112–125; doi: 10.1007/s10787-007-0021-x.

[5] W.F. Kean, L. Hart, W.W. Buchanan, Br. J. Rheumatol. 36 (1997) 560–572; doi:10.1093/rheumatology/36.5.560.

[6] R. Eisler, Inflamm. Res. 52 (2003) 487–501; doi:10.1007/s00011-003-1208-2.

[7] I. Ott, Coord. Chem. Rev. 253 (2009) 1670-1681; doi:10.1016/j.ccr.2009.02.019.

[8] V. Milacic, Q.P. Dou, Coord. Chem. Rev. 253 (2009) 1649-1660; doi:10.1016/j.ccr.2009.01.032.

[9] M. Mphahlele, M. Papathanasopoulos, M.A. Cinellu, M. Coyanis, S. Mosebi, T. Traut, R. Modise, J. Coates, R. Hewer, Bioorg. Med. Chem. 20 (2012) 401-407; doi:10.1016/j.bmc.2011.10.072.

[10] L. Ronconi, L. Giovagnini, C. Marzano, F. Bettio, R. Graziani, G. Pilloni, D. Fregona, Inorg. Chem. 44 (2005) 1867-1881; doi:10.1021/ic048260v.

[11] V. Milacic, D. Chen, L. Ronconi, K.R. Landis-Piwowar, D. Fregona, Q.P. Dou, Cancer Res. 66 (2006) 10478-10486; doi:10.1158/0008-5472.CAN-06-3017.

[12] R.V. Parish, B.P. Howe, J.P. Wright, J. Mack, R.G. Pritchard, Inorg. Chem. 35 (1996) 1659-1666; doi:10.1021/ic950343b.

[13] R.G. Buckley, A.M. Elsome, S.P. Fricker, G.R. Henderson, B.R.C. Theobald, R.V. Parish, B.P. Howe, L.R. Kelland, J. Med. Chem. 39 (1996) 5208-5214; doi:10.1021/jm9601563.

[14] R. Wai-Yin Sun, C.-M. Che, Coord. Chem. Rev. 253 (2009) 1682-1692; doi:10.1016/j.ccr.2009.02.017.

[15] Y.F. To, R. W.-Y. Sun, Y. Chen, V.S.-F. Chan, W.-Y. Yu, P.K.-H. Tam, C.-M. Che, C.-L.S. Lin, Int. J. Cancer 124 (2009) 1971-1979; doi:10.1002/ijc.24130.

[16] P.J. Davies, Plant Hormones, Springer, Dordrecht, Netherlands, 1997.

[17] L. Meijer, A. Borgne, O. Mulner, J.P.J. Chong, J.J. Blow, N. Inagaki, M. Inagaki, J.G. Delcros, J.P. Moulinoux, Eur. J. Biochem. 243 (1997) 527−536; doi:10.1111/j.1432-1033.1997.t01-2-00527.x.

[18] C. Benson, S. Kaye, P. Workman, M. Garret, M. Walton, J. de Bono, Br. J. Cancer 92 (2005) 7−12; doi:10.1038/sj.bjc.6602229.

[19] R. Vrzal, P. Štarha, Z. Dvořák, Z. Trávníček, J. Inorg. Biochem. 104 (2010) 1130−1132; doi:10.1016/j.jinorgbio.2010.07.002.

[20] Z. Trávníček, M. Matiková -Maľarová, R. Novotná, J. Vančo, K. Štěpánková, P. Suchý, J. Inorg. Biochem. 105 (2011) 937−948; doi:10.1016/j.jinorgbio.2011.04.002.

[21] P. Štarha, Z. Trávníček, R. Herchel, I. Popa, P. Suchý, J. Vančo, J. Inorg. Biochem. 103 (2010) 432−440; doi:10.1016/j.jinorgbio.2008.12.009.

[22] Z. Trávníček, P. Štarha, J. Vančo, T. Šilha, J. Hošek, P. Suchý, G. Pražanová, J. Med. Chem. 55 (2012) 4568-4579; doi:10.1021/jm201416p.

[23] J.A. Kuhnle, G. Fuller, J. Corse, B.E. Mackey, Physiol. Plantarum 41 (1977) 14–21; doi:10.1111/j.1399-3054.1977.tb01514.x.

[24] W. Schöniger, Mikrochim. Acta 44 (1956), 869–876; doi:10.1007/BF01262130.

[25] M. Zimmermann, Pain 16 (1983) 109-110; doi:10.1016/0304-3959(83)90201-4.

[26] H.Y. Chang, M.J. Sheu, C.H. Yang, Z.C. Leu, Y.S. Chang, W.H. Peng, S.S. Huang, G.J. Huang, Evidence-Based Compl. Altern. Med. (2011), Article ID 478246; doi:10.1093/ecam/nep027.

[27] C.J. Pouchert, The Aldrich Library of Infrared Spectra, Aldrich Chemical Company Press, Milwaukee, USA, 1981.

[28] K. Nakamoto, Infrared Spectra of Inorganic and Coordination Compounds, J. Wiley and Sons, New York, USA, 1997.

[29] S.S. Al-Jaroudi, M. Fettouhi, M.I.M. Wazeer, A.A. Isab, S. Altuwaijri, Polyhedron 50 (2013) 434-442; doi: 10.1016/j.poly.2012.11.034.

[30] A.Schimanski, E. Freisinger, A. Erxleben, B. Lippert, Inorg. Chim. Acta 283 (1998) 223–232; doi:10.1016/S0020-1693(98)00099-1.

[31] U. Abram, J. Mack, K. Ortner, M. Müller, J. Chem. Soc. Dalton Trans. (1998) 1011–1019; doi:10.1039/A708618K.

[32] C.M. Mikulski, D. Braccia, D. Delacato, J. Fleming, D. Fleming, Inorg. Chim. Acta 106 (1985) L13–L15; doi:10.1016/S0020-1693(00)87546-5.

[33] N.V. Hud (ed.), Nucleic Acid-Metal Ion Interactions, RSC Publishing, Cambridge, UK, 2009.

[34] A.D. Becke, J. Chem. Phys. 98 (1993) 1372−1377; doi:10.1063/1.464304.

[35] V. Rassolov, J.A. Pople, M. Ratner, P.C. Redfern, L.A. Curtiss, J. Comput. Chem. 22 (2001) 976−984; doi:10.1002/jcc.1058.

[36] V. Shao, L.F. Molnar, Y. Jung, J. Kussmann, C. Ochsenfeld, S.T. Brown, A.T.B. Gilbert, L.V. Slipchenko, S.V. Levchenko, D.P. O'Neill, R.A. DiStasio, Jr., R.C. Lochan, T. Wang, G.J.O. Beran, N.A. Besley, J.M. Herbert, C.Y. Lin, T. Van Voorhis, S.H. Chien, A. Sodt, R.P. Steele, V.A. Rassolov, P.E. Maslen, P.P. Korambath, R.D. Adamson, B. Austin, J. Baker, E.F.C. Byrd, H. Dachsel, R.J. Doerksen, A. Dreuw, B.D. Dunietz, A.D. Dutoi, T.R. Furlani, S.R. Gwaltney, A. Heyden, S. Hirata, C.P. Hsu, G. Kedziora, R.Z. Khalliulin, P. Klunzinger, A.M. Lee, M.S. Lee, W.Z. Liang, I. Lotan, N. Nair, B. Peters, E.I. Proynov, P.A. Pieniazek, Y.M. Rhee, J. Ritchie, E. Rosta, C.D. Sherrill, A.C. Simmonett, J.E. Subotnik, H.L. Woodcock III, W. Zhang, A.T. Bell, A.K. Chakraborty, D.M. Chipman, F.J. Keil, A. Warshel, W.J. Hehre, H.F. Schaefer, J. Kong, A.I. Krylov, P.M.W. Gill, M. Head-Gordon, Phys. Chem. Chem. Phys. 8 (2006) 3172−3191; doi:10.1039/B517914A.

[37] F.H. Allen, Acta Cryst. B 58 (2002) 380–388; doi:10.1107/S0108768102003890.

[38] H. Sivaram, J. Tan, H.V. Huynh, Organometallics 31 (2012) 5875-5883; doi:10.1021/om300444c.

Table 1. Selected coordination shifts ($\Delta\delta = \delta_{complex} - \delta_{ligand}$, ppm) calculated from ^{1}H and ^{13}C NMR spectra for the gold(III) complexes **1–5**.

Complex	^{1}H NMR		^{13}C NMR				
	C2H	C8H	C2	C6	C5	C4	C8
1	-0.12	-0.28	-1.64	0.30	1.78	-6.44	8.42
2	-0.12	-0.32	-1.69	0.22	1.35	-10.27	8.33
3	-0.07	-0.17	-0.90	-0.20	1.01	-4.83	8.41
4	-0.09	-0.81	-0.72	-0.22	0.99	-6.98	8.75
5	-0.04	-0.79	-0.77	-0.32	1.39	-6.59	8.86

Figure/Scheme Legends

Scheme 1. Schematic representation of the synthesis of gold(III) complexes (**1**–**5**) and the *N*6-benzyladenine (HL1-5) derivatives given with the atom numbering scheme of the organic compounds.

Fig. 1 Geometry of [Au(HL1)Cl_3] (**1**) optimized at the B3LYP/LACVP+* level of theory.

Fig. 2. Effects of the tested complexes (**1**–**5**), N6-benzyladenine derivatives used as ligands (HL1–HL5), $AuCl_3$, and the reference drug prednisone (**Pred.**) on the LPS-induced TNF-α secretion in macrophages derived from the THP-1 cell line. Cells were pre-treated with the compounds (5 μM), or the vehicle (**Veh.**; DMSO) only. After 1 h of incubation, the inflammatory response was induced by LPS [except for the control cells (**CTRL**)]. The results are expressed as means ± S.E. for three independent experiments. * significant difference in comparison to vehicle-treated cells ($P<0.05$), ** significant difference in comparison to vehicle-treated cells ($P<0.01$).

Fig. 3 A time-dependent profile of anti-oedematous activity of the tested compounds. A single asterisk besides the symbol for complex **1** at 300 min means that the applied dose of the complex led to toxic death of all laboratory animals behind this time-point.

Graphical abstract

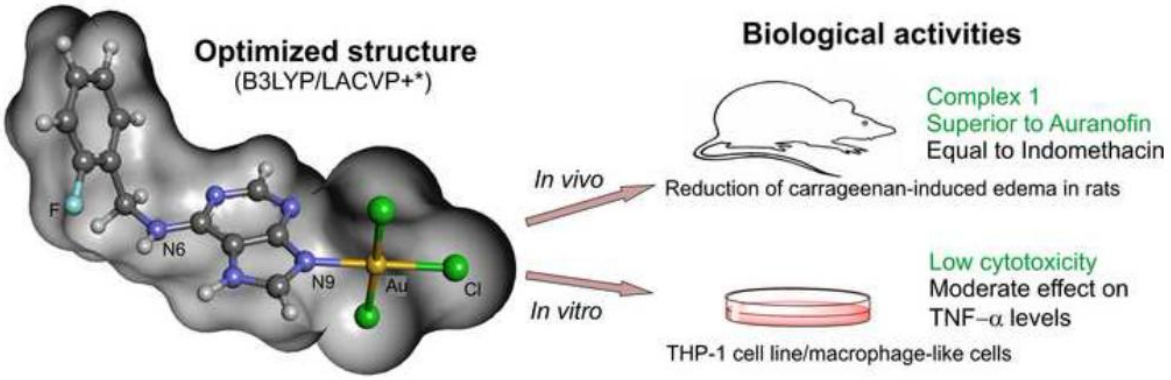

Synopsis:

Au(III) complexes of the type $[Au(HL1\text{-}5)Cl_3]\cdot nH_2O$ involving *N*6-benzyladenine derivatives were prepared and fully characterized. They showed negligible *in vitro* cytotoxicity, moderate *in vitro* anti-inflammatory activity on LPS-activated THP-1 macrophages, and significant *in vivo* anti-oedematous activity, even exceeding the activity of gold-containing metallodrug Auranofin.

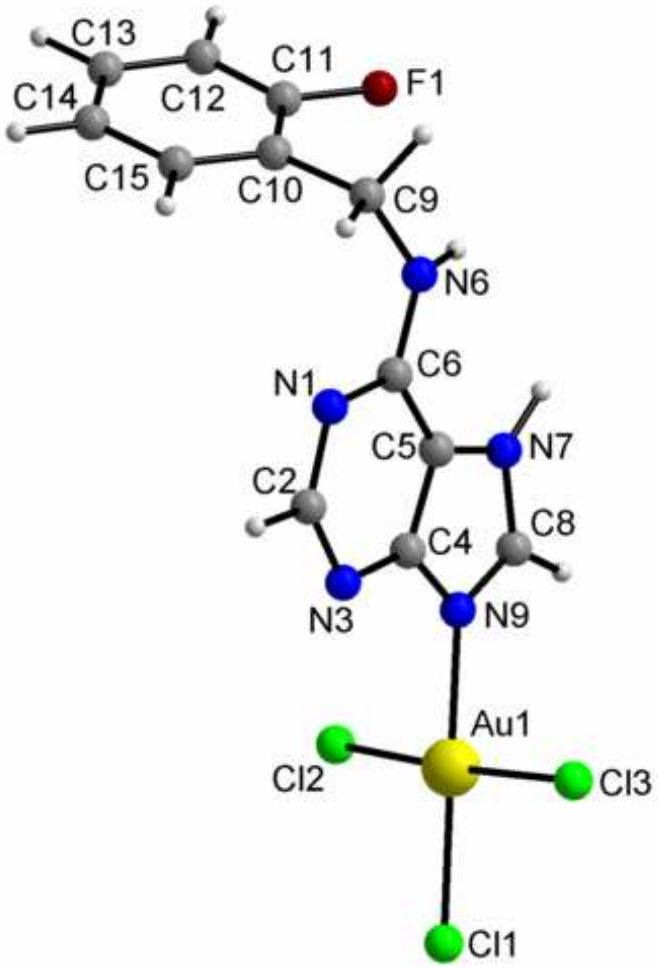

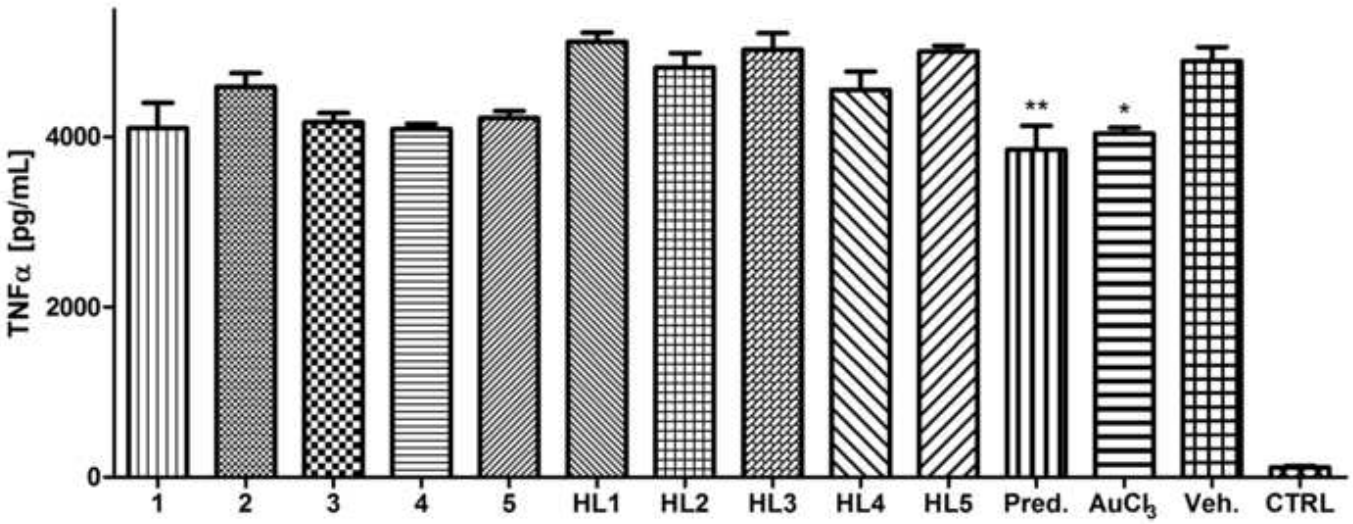

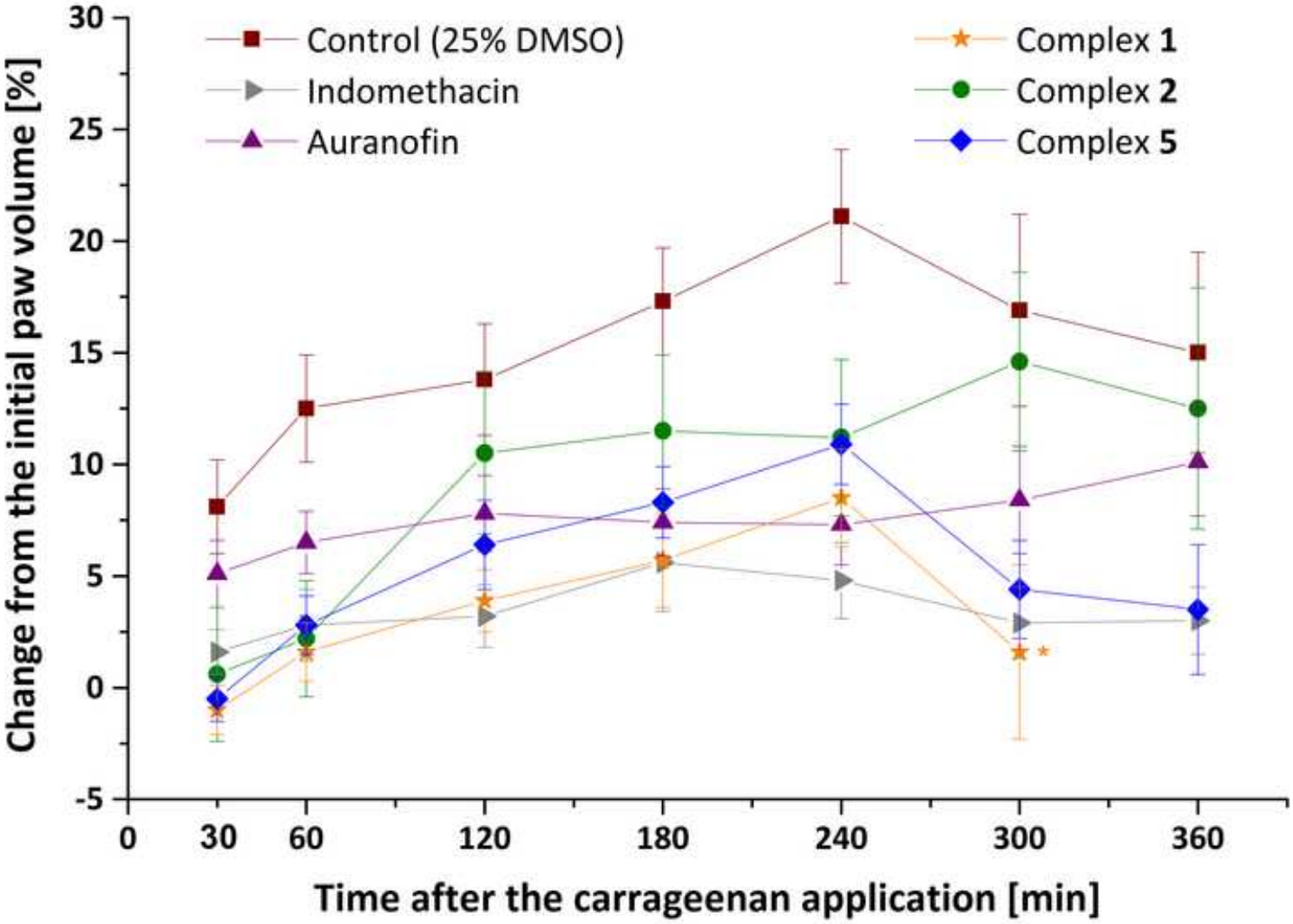

Highlights:

- [Au(HL1-5)Cl_3]·*n*H_2O complexes with *N*6-benzyladenine derivatives (HL1-5) are reported
- Low cytotoxicity against human monocytic cell line THP-1
- Moderate *in vitro* anti-inflammatory activity
- *In vivo* anti-inflammatory activity higher than metallodrug Auranofin